D.O. SAVCHENKO,[1] D.A. IAKUBOVSKYI [2,1]
[1] Bogolyubov Institute for Theoretical Physics
(14b, Metrolohichna Str., Kyiv 03143, Ukraine; e-mail: dsavchenko@bitp.kiev.ua)
[2] Discovery Center, Niels Bohr Institute
(17, Blegdamsvej, Copenhagen, Denmark)

UDC 524.8

TOWARD ROBUST DETECTION OF A FAINT NARROW LINE IN X-RAYS – THE ROLE OF CONTINUUM-INDUCED SYSTEMATICS

Some of recent detections of a narrow emission line at ∼3.5 keV have been accompanied by subsequent non-detections in the same sources, raising discussion about the actual level of systematic errors. In this paper, we study the systematics caused by an imperfect knowledge of a continuum model. Our simple theoretical estimate and detailed modeling of simulated spectra allow us to calculate the value of this "continuum-induced" systematics for the first time. We show that, for some objects such as the M31 central part or the Draco dwarf spheroidal galaxy, the obtained level of systematics within a well-defined continuum model allows one to fully reconcile the controversial results claimed previously by different groups of authors. To minimize the effect of "continuum-induced" systematics, we show that one should reasonably decrease the size of the spectral bin and increase the modeled energy range.

Keywords: X-rays, general line, identification of the dark matter.

1. Introduction

Detecting faint narrow spectral features in continuum spectra is a long-standing problem in astronomy, see e.g. [1–8]. The particular case of our interest is the search for the dark matter decay line in X-rays. According to the recent review [9], the most promising line as a candidate representing the radiatively decaying dark matter in X-rays is the unidentified narrow emission line at ∼3.5 keV. Bulbul *et al.* [10] reported this line in the stacked spectra of nearby galaxy clusters observed by the *XMM-Newton* X-ray observatory [11] and in the central part of the Perseus cluster observed by the *XMM-Newton* and *Chandra* [12] X-ray observatories. Boyarsky *et al.* [13] reported the presence of this line in the central part of the Andromeda galaxy and in the Perseus cluster outskirts observed by *XMM-Newton*. At the moment, there is an apparent inconsistency between the results about the flux and significance of the ∼3.5 keV line claimed by different groups. For example, the authors in [14] have found a much less significant line in the Andromeda galaxy using the same dataset as [13], see also [15, 16] for discussion. Two recent papers [17, 18] reported controversial results about the presence of the ∼3.5 keV line in a prolonged *XMM-Newton* observation of the Draco dwarf spheroidal galaxy. Jeltema and Profumo [17] find no evidence for the line in both imaging spectrometers on-board *XMM-Newton* – MOS [19] and PN [20]. Ruchayskiy *et al.* [18] reported the presence of a line-like feature in PN (but not in MOS) with properties expected from the decaying dark matter hypothesis. The further detection of ∼3.5keV line in *Suzaku* [21] observations of the central part of the Perseus cluster by [22, 23] is followed by a non-detection claims using *Suzaku* [24] and *Hitomi* data [25]. In addition, while [26] reported the presence of a weak (2σ) line in a stacked *Suzaku* dataset of galaxy clusters, [27,28] have not detected the line at ∼3.5 keV using different combined samples of dark matter-dominated objects observed by *XMM-Newton* and *Chandra*, respectively, although [26–28] reported that the statistics and (for the sample of [27]) the total exposure time of the datasets used in their analysis are much less as compared to [10].

The aim of this paper is to address *some of* the above-mentioned controversies about the (non-)detection of faint narrow spectral features in more details. In Sec. 2, we identify the origin of the "continuum-induced" systematics, which should be taken into account when searching for a faint narrow spectral feature, and derive the simple analytic expression to estimate its numerical value. In Sec. 3, we develop a more detailed estimate based on a set of dedicated numerical simulations of X-ray spectra for objects of our interest. In Sec. 4, we present our results summarized in Table 2 and able to resolve some of the apparent controversies between the claims of different groups about the fluxes and significances of the ∼3.5 keV line: namely, in the central part of the Andromeda galaxy [13, 14], the central part of the Perseus galaxy cluster [10, 22–24, 29], and the Draco dwarf spheroidal galaxy [17, 18]. Finally, in Sec. 5, we discuss our results.

2. Simple Analytic Estimate

To estimate the value of the continuum-induced systematics, we assume a flat featureless continuum X-ray spectrum [1] observed during the exposure time $T_{\rm exp}$ by an instrument with energy resolution $\Delta E_{\rm line}$ and effective area $A_{\rm eff}$.

Being modeled over the energy range ΔE, it corresponds to n spectral bins given the bin size $E_{\rm bin} = \Delta E/n$. The difference of χ^2 statistics between the actual and best-fit models is given by

$$\Delta\chi^2 \equiv \chi^2_{\rm actual} - \chi^2_{\rm best\text{-}fit} = \sum_{i=1}^{n} \frac{(N_{{\rm mod},i} - N_i)^2}{N_i}. \qquad (1)$$

Here, we assume $\Delta\chi^2 = 9$, which corresponds to, e.g., 3σ significance for 1 extra degree of freedom, 2.5σ for 2 extra degrees of freedom, *etc.*

[1] Note that the results obtained in this section are very general and can be directly applied not only to X-rays, but also to other energy ranges of electromagnetic radiation (such as optical, UV, and γ-rays), as well as to other species of detected particles (such as cosmic rays and neutrinos),

By assuming that the continuum changes by *the same* ratio for all bins [2], i.e., $N_{{\rm mod},i}/N_i = {\rm const}$, where $N_i = T_{\rm exp} F_{{\rm cont},i} E_{\rm bin}$ is the number of continuum counts in the i-th bin, $N_{{\rm mod},i}$ is the number of modeled continuum counts in the same bin, we get

$$N_{{\rm mod},i} - N_i = \frac{3}{C_{\rm cont} T_{\rm exp}} N_i.$$

Here, $C_{\rm cont} = \sum N_i T_{\rm exp}$ is the total continuum rate (in cts/s) over the whole modeling range, and the factor 3 comes from the chosen value of $\sqrt{\Delta\chi^2}$. Then the difference in line counts will be

$$\Delta N_{\rm line} \equiv \sum_{\rm line} (N_{{\rm mod},i} - N_i) = 3\frac{F_{\rm cont}\Delta E_{\rm line} T_{\rm exp}}{C_{\rm cont} T_{\rm exp}},$$

and the uncertainty on the line flux $\Delta F_{\rm line,est}$ ph/cm^2/s is estimated as

$$\Delta F_{\rm line,est} \simeq 3\frac{\Delta E_{\rm line}}{A_{\rm eff}} \times \frac{F_{\rm cont}}{T_{\rm exp}^{1/2} C_{\rm cont}^{1/2}}, \qquad (2)$$

where $F_{\rm cont}$ is the continuum level [3] (in cts/s/keV) near the line. Note that Eq. (2) is valid for statistically independent bins, which is true, if the minimal number of counts per spectral bin is larger than 20, so the usage of χ^2 statistics is justified, see, e.g., Sec. 6.5 of [30] for details.

As a result, to decrease $\Delta F_{\rm line,est}$, one needs to:

1. increase the energy resolution (scales as $\Delta E_{\rm line}$);
2. increase the effective area (scales as $A_{\rm eff}^{-1}$);
3. increase the observation exposure time (scales as $T_{\rm exp}^{-1/2}$);
4. decrease the continuum level (scales as $F_{\rm cont}/C_{\rm cont}^{1/2}$);
5. increase the modeled energy range (scales as $C_{\rm cont}^{-1/2}$).

The first two options can be reached by new better instruments, for example, *Micro-X* sounding rocket experiment [31], Soft X-ray spectrometer (SXS) [32]

[2] Figure 1 shows that this assumption works reasonably well for objects modeled by a single continuum folded with instrumental response, such as M31 center; for more complex continuum models (e.g., the 2-component model of Draco dSph), this clearly gives us an underestimate, and detailed simulations should be performed instead.

[3] Note that if one redefines $F_{\rm cont} = f_{\rm cont} A_{\rm eff}$ (as it should be, if cosmic radiation dominates the background rate), the estimated value $\Delta F_{\rm line,est}$ given by Eq. (2) will be proportional to $(A_{\rm eff} T_{\rm exp})^{-1/2}$, similarly to expectations.

Table 1. **The models used when fitting the simulated data**

Object	Fitting interval, keV	*Xspec* model	Values of continuum parameters
M31	2–2.7, 3–8.1	Model 1: sky gaussian + plaw35 Model 2: back plaw35	PhoIndex = 1.706, norm = $1.17 \times 10^{-3}\ \frac{\mathrm{ph}}{\mathrm{cm^2 s\,keV}}$ PhoIndex = 0.397, norm = $0.0585 \frac{\mathrm{ph}}{\mathrm{s\,keV}}$
M31	3–4	Model 1: sky gaussian Model 2: back plaw35	 PhoIndex = 1.414, norm = $0.4 \frac{\mathrm{ph}}{\mathrm{s\,keV}}$
Draco	2.4–7, 10–11	Model 1: sky phabs*cflux*powerlaw + + gaussian Model 2: back plaw35	nH = $0.0225 \times 10^{22}\ \frac{\mathrm{atoms}}{\mathrm{cm^2}}$, PhoIndex = 1. 59 lg10flux = $0.32 \times 10^{-11}\ \frac{\mathrm{erg}}{\mathrm{cm^2 s}}$ PhoIndex = 0.355, norm = $0.1919\ \frac{\mathrm{ph}}{\mathrm{s\,keV}}$
Draco	2.5–5	Model 1: sky gauss Model 2: back plaw35	 PhoIndex = 0.55, norm = $0.24 \frac{\mathrm{ph}}{\mathrm{s\,keV}}$

Table 2. **A summary of the ∼3.5 keV line flux (F_{line}) measurements and calculations of the continuum-induced systematics for the central part of the Andromeda galaxy and the Draco dwarf spheroidal galaxy, based on our estimate Eq. (2) ($\Delta F_{\mathrm{line,est}}$) and detailed simulations described in Sec. 3 (ΔF_{line}) analyzed in this paper**

Reference for F_{line} measurement	F_{line}, 10^{-6} ph/cm^2/s	ΔE, keV	E_{bin}, eV	$\Delta F_{\mathrm{line,est}}$, 10^{-6} ph/cm^2/s	ΔF_{line}, 10^{-6} ph/cm^2/s
M31, 14’ circle, *XMM-Newton*/MOS, see left Fig. 1					
Boyarsky *et al.* [13]	$4.9^{+1.6}_{-1.3}$	8.0	60	0.56	0.9
Jeltema and Profumo [14]	$2.1^{+1.5}_{-1.5}$	1.0	5	1.16	1.5
Draco dwarf spheroidal galaxy, 14’ circle, *XMM-Newton*/PN, see right Fig. 1					
Ruchayskiy *et al.* [18]	$1.65^{+0.67}_{-0.70}$	5.6	65	0.22	0.45
Jeltema and Profumo [17]	$\lesssim 2.5$	2.5	5	0.31	0.72

on-board *Hitomi* (former *Astro-H*) mission [33] [4], X-ray Integral Field Unit (X-IFU) [35, 36] on-board planned *Athena* mission [37,38], the *eROSITA* instrument on-board planned *Spektrum-Röntgen-Gamma* mission [39], and the Large Area Detector (LAD) on-board proposed *LOFT* mission [40], see also [41–49] for more details. The next two possibilities can be addressed by prolonged observations (with larger T_{exp}) of fainter objects (with both smaller F_{cont} and C_{cont}). Finally, the last option depends *entirely* on our modeling procedure and thus can be optimized *without* choosing new instruments and/or observations.

3. Simulations

To precisely calculate the values of ΔF_{line}, we performed a dedicated set of simulations of spectra from objects of our interest, see Table 2. The corresponding *XMM-Newton* and *Suzaku* best-fit models and instrumental responses were taken from actual spectra of [13, 18, 29] and [23], respectively.

The used models are summarized in Table 1. The added line had the normalization of $3 \times \times 10^{-5}\,\mathrm{ph\,cm^{-2}\,s^{-1}}$ and the position at 3.55 keV. Gaussian line *Sigma* is fixed at 0.001 keV value. The gaussian fit parameters were chosen correspondingly. The model definitions are given in *Xspec* notation. The *plaw35* model is the redefined *powerlaw* model with the normalization given at 3.5 keV. In each simulation, the first model component is folded with instrumental response, while the second one is unfolded. When modeling over the wide energy range, the second model component accounts for the instrumental response. The modeling in a narrow energy range, as was used in [14, 17] is, in general, not physically motivated, and the unfolded component de-

[4] Before being broken apart, *Hitomi* has already observed the Perseus cluster [25, 34].

 ISSN 0372-400X. Укр. фіз. журн. 2017. Т. 62, № 7

scribes the general continuum behavior. We do not include the other astrophysical lines in the simulation procedure, because there is no strong lines in modeled objects in the region of interest, so this will not affect the obtained results.

By using the *fakeit* procedure from *PyXspec* v. 1.1.0 [50], we generated 100 independent realizations of X-ray spectra for each object, added the specially generated spectrum from a narrow emission line located at 3.5 keV to them, and re-grouped the obtained spectra by larger spectral bins with the help *grppha* v.3.0.1, a part of HEASOFT v. 6.18. For each simulation, we allowed the number of counts in each bin to vary among the realizations according to the Gaussian distribution [5]. All simulated spectra were then modeled with the same best-fit continuum model, by using the energy range ΔE indicated in Table 2. The model parameters are then calculated in *Xspec* by minimizing the total χ^2 of the fit. After that, we calculated maximal variations of the continuum normalization at 3.5 keV allowed by the $\Delta\chi^2 = 9$, by using *steppar* procedure of *PyXspec*, and the minimal and maximal best-fit normalizations of *Gaussian* component corresponding to extreme variations of the background continuum (which is the sum of cosmic and instrumental background components and the source emission component). Finally, we derive the value of $\Delta F_{\rm line}$ as the semidifference between the largest and smallest best-fit normalizations of the *Gaussian* component averaged through 100 independent realizations.

4. Results and Conclusions

Our main results are summarized in Table 2, which contains information about the reported measurement of the $\sim$3.5 keV line flux ($F_{\rm line}$), and calculations of continuum-induced systematics based on our estimate Eq. (2) ($\Delta F_{\rm line,est}$) and detailed simulations described in Sec. 3 ($\Delta F_{\rm line}$). As one can see, the resulting values of $\Delta F_{\rm line}$ obtained for the M31 central part by *XMM-Newton*/MOS cameras and the Draco dwarf spheroidal galaxy by *XMM-Newton*/PN camera allow us to reconcile the positive detections of [13, 18] with corresponding non-detections of [14,17]. Because the values of $\Delta F_{\rm line}$ obtained for non-detections of [14, 17] are significantly larger than the corresponding values of $\Delta F_{\rm line}$ obtained for detections of [13,18] (mostly, due to a much smaller modeled energy range ΔE used in [14, 17], as Eq. (2) demonstrates), we conclude that the fact of positive detections of [13, 18] is not affected by the presence of the continuum-induced systematics. On the contrary, taking this effect into account should significantly *weaken* the upper bounds on the dark matter decay lifetime inferred, e.g., by [17], by making them consistent with positive detections obtained by other groups. The fitting intervals used in simulations were chosen strictly the same as provided in Table 2. The other values of ΔE were not tested, since the direct investigation of the dependence of a systematics on the fitting interval is not our point. However, it was mentioned that the obtained level of the systematics is lower for wider fitting intervals.

In addition, Figure shows the values of $\Delta F_{\rm line}$ reconstructed from our simulations of the central part of the Andromeda galaxy and the Draco dwarf spheroidal galaxy (dSph), respectively. For both objects, the calculated values of $\Delta F_{\rm line}$ allow us to fully reconcile the new line detections claimed by [13, 18] with its non-detections claimed by different groups [14, 17]. Indeed, let us consider the measurement of $F_{\rm line,Draco,R15} = 1.65^{+0.67}_{-0.70} \times 10^{-6}{\rm ph/cm^2/s}$ in Draco dSph reported by [18]. By using reasonably wide spectral bins (65 eV per bin) and the modeled energy range, the results of [18] were affected by a relatively small value of the model-induced systematics, $\Delta F_{\rm line,Draco,R15} = 0.45 \times 10^{-6}{\rm ph/cm^2/s}$ (see the filled circle on the right of Figure, which constitutes only about 35% of their best-fit flux value or $\sim$0.8 of purely statistical errors. In contrast to that, much narrower spectral bins (5 eV per bin) and the modeled energy range were used in [17], which results in a much larger value of the systematics, $\Delta F_{\rm line,Draco,JP16} \simeq 0.72 \times 10^{-6}{\rm ph/cm^2/s}$, see the square on the right of Figure, which can easily "hide" the line observed by [18].

The same is true for the central observations of the Andromeda galaxy: while the result of [13], $F_{\rm line,M31,B14} = 4.9^{+1.6}_{-1.3} \times 10^{-6}{\rm ph/cm^2/s}$ remains practically unaffected by the continuum-induced systematics ($\Delta F_{\rm line,M31,B14} = 0.9 \times 10^{-6}{\rm ph/cm^2/s}$, see the filled circle on the left of Figure) due to their

[5] We have checked that the minimal number of counts per spectral bin in all spectra of our interest is larger than 20, so the distribution of counts is Gaussian, and the usage of χ^2 statistics is justified, see, e.g., Sec. 6.5 of [30] for details.

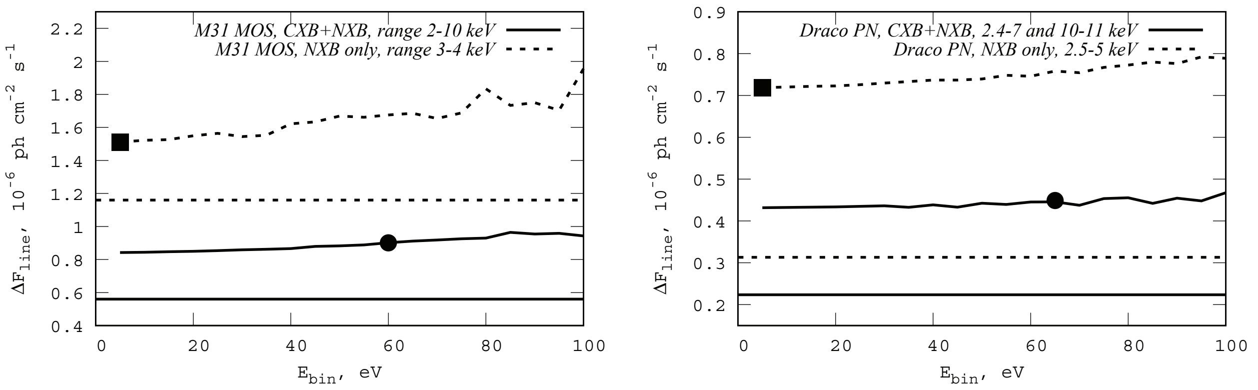

Mean fractional deviation $\Delta F_{\rm line}$ (solid lines) for the central part of the Andromeda galaxy observed by *XMM-Newton*/MOS [13–16] (*left*) and for the Draco dSph observed by *XMM-Newton*/PN camera [17, 18] (*right*), as a function of the spectral bin size $E_{\rm bin}$. The corresponding numerical estimates (independent of $E_{\rm bin}$) obtained from Eq. (2) are shown by horizontal dashed lines. Contrary to them, the values of $\Delta F_{\rm line}$ obtained from the simulations slightly grow with $E_{\rm bin}$, according to the expectations from [51]. Circles and squares denote the corresponding values of $\Delta F_{\rm line}$ for specific spectral bin sizes mentioned in Table 2

wide spectral bins (60 eV per bin) and the modeled energy range, the subsequent study of [14] claiming $F_{\rm line,M31,JP15} = (2.1 \pm 1.5) \times 10^{-6}{\rm ph/cm^2/s}$ is much stronger affected, $\Delta F_{\rm line,M31,JP15} = 1.5 \times 10^{-6}{\rm ph/cm^2/s}$, see also the square on the left of Figure.

$\Delta F_{\rm line}$ was obtained from simulations with fitting intervals just as those used in corresponding articles. As was mentioned, the wider the fitting interval, the lower the systematic error. As the main point of this article was to numerically quantify the uncertainty in those specific models, but not its strict dependence on ΔE, the additional fitting interval widths were not tested in our simulations. However, the dependence of the systematic uncertainty on the energy bin size was obtained in simulations and is provided in Figure.

Note that small energy bins are not statistically independent, because of a relatively poor energy resolution of instruments. The difference between the simple estimate from Eq. 2 and the simulated values can at least partially originate from this statistical dependence. The selection of $\Delta\chi^2 = 9$ is poorly motivated in this case. To account this, we have simulated 5000 samples of M31 spectra and have obtained best-fit values of the line normalization for each of them, using $\Delta E = 8$ keV, $\Delta E_{\rm line} = 5$ eV. The dispersion of the obtained values is equal to $\sim 10^{-6}$ ph cm^2 s^{-1}, which gives another estimate of $\Delta F_{\rm line}$ close to the value obtained in our analysis (0.84×10^{-6} ph cm^2 s^{-1}). Such estimation does not require an assumption on the statistical independence of energy bins.

5. Discussion

We identify the new source of systematics on the flux of the narrow X-ray line in background-dominated spectra. The origin of this "continuum-induced" systematics is a variance of the background modeling statistics, i.e. the background with slightly changed normalization is still allowed by the model statistics. In turn, this would affect the flux of the reported new line. By performing both simple estimates and detailed simulations, we show that this new type of the systematics is able to reconcile the controversial results on the Draco dwarf spheroidal galaxy (dSph) and the Andromeda galaxy obtained by different groups.

As Figure demonstrates, it is possible to decrease the level of "continuum-induced" systematics by applying smaller spectral bins (according to the effect described in [51]) and wider modeling energy ranges. However, both options should be used with caution. For example, using coarser spectral bins often helps to find a better continuum model due to the clearer visual inspection of adjacent line residuals. Similarly, the modeling range extension to the energies with large systematic uncertainties (e.g., dominated by bright or imperfectly modeled instrumental features) will decrease the quality of a fit and, as a result, the robustness of the obtained best-fit model.

Finally, it is important to note that the discrepancies between some measurements cannot be resolved, by using our method. The most important of them is the non-observations of 3.5 keV line in the Perseus cluster by *Suzaku* [24] and, more recently, *Hitomi* [25], which are apparently in conflict with other meaurements performed by *XMM-Newton* [10, 29], *Chandra* [10] and *Suzaku* [22,23]. For example, for the *Hitomi* observation of the 3.5 keV line, our estimate of the line uncertainty gives $\Delta F_{\text{line,est}} \simeq 2.8 \times 10^{-6}$ ph/cm^2/s, much smaller than the apparent discrepancy between *XMM-Newton*/MOS and *Hitomi*/SXS measurements, as Fig. 3 of [25] demonstrates. We will study the systematic effects in such objects in a separate study.

The authors thank E. Bulbul, J. Franse, and O. Ruchayskiy for the collaboration and useful comments. The work of D.I. was supported by a research grant from VILLUM FONDEN. The work of D.S. was supported partially by the Program of Cosmic Research of the National Academy of Sciences of Ukraine and the State Fund for Fundamental Research of Ukraine, grant F64/45-2016.

1. J. Truemper, W. Pietsch, C. Reppin, W. Voges, R. Staubert, E. Kendziorra. Evidence for strong cyclotron line emission in the hard X-ray spectrum of Hercules X-1. *Astrophys. J.* **219**, L105 (1978).
2. T.-P. Li, Y.-Q. Ma. Analysis methods for results in gammaray astronomy. *Astrophys. J.* **272**, 317 (1983).
3. R. Protassov, D.A. van Dyk, A. Connors, V.L. Kashyap, A. Siemiginowska. Statistics, handle with care: Detecting multiple model components with the likelihood ratio test. *Astrophys. J.* **571**, 545 (2002), astro-ph/0201547.
4. K. Nandra, P.M. O'Neill, I.M. George, J.N. Reeves. An XMM–newton survey of broad iron lines in Seyfert galaxies. *Mon. Not. R. Astr. Soc.* **382**, 194 (2007).
5. M.G. Malygin, D.A. Iakubovskyi. Search for cyclotron absorptions from > magnetars in the quiescence with XMM-Newton . In *Proceedings of the 17th Conference of Young Scientists*, edited by V. Choliy, G. Ivashchenko, and O. Ivaniuk (2011), p. 43.
6. M. Ackermann, M. Ajello, A. Albert, L. Baldini, G. Barbiellini, K. Bechtol, R. Bellazzini, B. Berenji, R.D. Blandford, E.D. Bloom *et al.* Fermi LAT search for dark matter in gamma-ray lines and the inclusive photon spectrum. *Phys. Rev. D 86*, 022002 (2012).
7. A. Abramowski, F. Acero, F. Aharonian, A. G. Akhperjanian, G. Anton, S. Balenderan, A. Balzer, A. Barnacka, Y. Becherini, J. Becker Tjus *et al.* Search for photonlinelike signatures from dark matter annihilations with H.E.S.S. *Phys. Rev. Lett.* **110**, 041301 (2013).
8. S. Campana, V. Braito, P. D'Avanzo, G. Ghirlanda, A. Melandri, A. Pescalli, O.S. Salafia, R. Salvaterra, G. Tagliaferri, S.D. Vergani. Searching for narrow absorption and emission lines in XMM-Newton spectra of gamma-ray bursts. *Astr. Astrophys.* **592**, A85 (2016).
9. D. Iakubovskyi. Observation of the new line at 3.55 keV in X-ray spectra of galaxies and galaxy clusters. *Adv. Astr. Space Phys.* **6**, 3 (2016).
10. E. Bulbul, M. Markevitch, A. Foster, R.K. Smith, M. Loewenstein, S.W. Randall. Detection of an unidentified emission line in the stacked X-ray spectrum of galaxy clusters. *Astrophys. J.* **789**, 13 (2014).
11. F. Jansen, D. Lumb, B. Altieri, J. Clavel, M. Ehle, C. Erd, C. Gabriel, M. Guainazzi, P. Gondoin, R. Much *et al.* XMM-Newton observatory. I. The spacecraft and operations. *Astr. Astrophys.* **365**, L1 (2001).
12. M.C. Weisskopf, H.D. Tananbaum, L.P. Van Speybroeck, S.L. O'Dell. Chandra X-ray observatory (CXO): Overview. In *X-Ray Optics, Instruments, and Missions III*, edited by J.E. Truemper and B. Aschenbach. *Proc. SPIE* **4012**, 2 (2000); astro-ph/0004127.
13. A. Boyarsky, O. Ruchayskiy, D. Iakubovskyi, J. Franse. Unidentified line in X-ray spectra of the Andromeda galaxy and Perseus galaxy cluster. *Phys. Rev. Lett.* **113**, 251301 (2014).
14. T. Jeltema, S. Profumo. Discovery of a 3.5 keV line in the Galactic Centre and a critical look at the origin of the line across astronomical targets. *Mon. Not. R. Astr. Soc.* **450**, 2143 (2015).
15. A. Boyarsky, J. Franse, D. Iakubovskyi, O. Ruchayskiy. Comment on the paper "Dark matter searches going bananas: The contribution of potassium (and chlorine) to the 3.5 keV line" by T. Jeltema and S. Profumo. e-prints http://adsabs.harvard.edu/abs/ 2014arXiv1408.4388B (2014).
16. T. Jeltema, S. Profumo. Reply to two comments on "Dark matter searches going bananas: The contribution of potassium (and chlorine) to the 3.5 keV line". e-prints http://adsabs.harvard.edu/abs/ 2014arXiv1411.1759J (2014).
17. T. Jeltema, S. Profumo. Deep XMM observations of Draco rule out at the 99 per cent confidence level a dark matter decay origin for the 3.5 keV line. *Mon. Not. R. Astr. Soc.* **458**, 3592 (2016).
18. O. Ruchayskiy, A. Boyarsky, D. Iakubovskyi, E. Bulbul, D. Eckert, J. Franse, D. Malyshev, M. Markevitch, A. Neronov. Searching for decaying dark matter in deep XMM–Newton observation of the Draco dwarf spheroidal. *Mon. Not. R. Astr. Soc.* **460**, 1390 (2016).
19. M.J.L. Turner, A. Abbey, M. Arnaud, M. Balasini, M. Barbera, E. Belsole, P.J. Bennie, J.P. Bernard, G.F. Bignami, M. Boer *et al.* The European photon imaging camera on XMM-Newton: The MOS cameras: The MOS cameras. *Astr. Astrophys.* **365**, L27 (2001), astro-ph/0011498.
20. L. Strüuder, U. Briel, K. Dennerl, R. Hartmann, E. Kendziorra, N. Meidinger, E. Pfeffermann, C. Reppin,

B. Aschenbach, W. Bornemann *et al.* The European photon imaging camera on XMM-Newton: The pn-CCD camera. *Astr. Astrophys.* **365**, L18 (2001).
21. K. Mitsuda, M. Bautz, H. Inoue, R.L. Kelley, K. Koyama, H. Kunieda, K. Makishima, Y. Ogawara, R. Petre, T. Takahashi *et al.* The X-ray observatory Suzaku. *Publ. Astr. Soc. Jap.* **59**, 1 (2007).
22. O. Urban, N. Werner, S. W. Allen, A. Simionescu, J.S. Kaastra, L.E. Strigari. A Suzaku search for dark matter emission lines in the X-ray brightest galaxy clusters. *Mon. Not. R. Astr. Soc.* **451**, 2447 (2015).
23. J. Franse, E. Bulbul, A. Foster, A. Boyarsky, M. Markevitch, M. Bautz, D. Iakubovskyi, M. Loewenstein, M. McDonald, E. Miller *et al.* Radial profile of the 3.55 keV line out to R_200 in the Perseus cluster. *Astrophys. J.* **829**, 124 (2016).
24. T. Tamura, R. Iizuka, Y. Maeda, K. Mitsuda, N.Y. Yamasaki. An X-ray spectroscopic search for dark matter in the Perseus cluster with Suzaku. *Publ. Astr. Soc. Jap.* **67**, 23 (2015).
25. Hitomi Collaboration, F. A. Aharonian, H. Akamatsu, F. Akimoto, S. W. Allen, L. Angelini, K. A. Arnaud, M. Audard, H. Awaki, M. Axelsson *et al.* Hitomi constraints on the 3.5 keV line in the Perseus galaxy cluster. *Astrophys. J.* **837**, L15 (2017).
26. E. Bulbul, M. Markevitch, A. Foster, E. Miller, M. Bautz, M. Loewenstein, S.W. Randall, R.K. Smith. Searching for the 3.5 keV line in the stacked Suzaku observations of galaxy clusters. *Astrophys. J.* **831**, 55 (2016).
27. F. Mernier, J. de Plaa, C. Pinto, J.S. Kaastra, P. Kosec, Y.-Y. Zhang, J. Mao, N. Werner. On the origin of central abundances in the hot intra-cluster medium – I. Individual and average abundance ratios from XMM-Newton EPIC. *Astr. Astrophys.* **592**, A157 (2016).
28. F. Hofmann, J.S. Sanders, K. Nandra, N. Clerc, M. Gaspari. 7.1 keV sterile neutrino constraints from X-ray observations of 33 clusters of galaxies with Chandra ACIS. *Astr. Astrophys.* **592**, A112 (2016).
29. D. Iakubovskyi, E. Bulbul, A.R. Foster, D. Savchenko, V. Sadova. Testing the origin of $\sim$3.55 keV line in individual galaxy clusters observed with XMM-Newton. e-prints http://adsabs.harvard.edu/abs/ 2015arXiv150805186I (2015).
30. P.R. Bevington, D.K. Robinson. Data reduction and error analysis for the physical sciences. 3rd ed. (McGraw-Hill, 2003) [ISBN: 0-07-247227-8].
31. E. Figueroa-Feliciano, A.J. Anderson, D. Castro, D.C. Goldfinger, J. Rutherford, M.E. Eckart, R.L. Kelley, C.A. Kilbourne, D. McCammon, K. Morgan *et al.* Searching for kev sterile neutrino dark matter with X-ray microcalorimeter sounding rockets. *Astrophys. J.* **814**, 82 (2015).
32. T. Takahashi, K. Mitsuda, R. Kelley, F. Aharonian, H. Akamatsu, F. Akimoto, S. Allen, N. Anabuki, L. Angelini, K. Arnaud *et al.* The ASTRO-H X-ray astronomy satellite. In *Society of Photo-Optical Instrumentation Engineers (SPIE), Conference Series* (2014), vol. 9144 of Society of Photo-Optical Instrumentation Engineers (SPIE) Conference Series, p. 25.
33. K. Mitsuda, R.L. Kelley, H. Akamatsu, T. Bialas, K.R. Boyce, G. V. Brown, E. Canavan, M. Chiao, E. Costantini, J.-W. den Herder *et al.* Soft X-ray spectrometer (SXS): the high-resolution cryogenic spectrometer onboard ASTRO-H. in *Society of Photo-Optical Instrumentation Engineers (SPIE), Conference Series* (2014), vol. 9144, p. 2.
34. Hitomi Collaboration, F. Aharonian, H. Akamatsu, F. Akimoto, S. W. Allen, N. Anabuki, L. Angelini, K. Arnaud, M. Audard, H. Awaki *et al.* The quiescent intracluster medium in the core of the Perseus cluster. *Nature* **535**, 117 (2016).
35. D. Barret, J.W. den Herder, L. Piro, L. Ravera, R. Den Hartog, C. Macculi, X. Barcons, M. Page, S. Paltani, G. Rauw *et al.* The hot and energetic universe: The X-ray integral field unit (X-IFU) for athena+. e-prints http://adsabs.harvard.edu/abs/2013arXiv1308.6784B (2013).
36. L. Ravera, D. Barret, J.W. den Herder, L. Piro, R. Clédassou, E. Pointecouteau, P. Peille, F. Pajot, M. Arnaud, C. Pigot *et al.* The X-ray integral field unit (X-IFU) for athena. In *Society of Photo-Optical Instrumentation Engineers (SPIE), Conference Series* (2014), vol. 9144, p. 2.
37. K. Nandra, D. Barret, X. Barcons, A. Fabian, J.-W. den Herder, L. Piro, M. Watson, C. Adami, J. Aird, J.M. Afonso *et al.* The hot and energetic Universe: A white paper presenting the science theme motivating the athena+ mission. e-prints http://adsabs.harvard.edu/abs/2013arXiv1306.2307N (2013).
38. D. Barret, K. Nandra, X. Barcons, A. Fabian, J.W. den Herder, L. Piro, M. Watson, J. Aird, G. Branduardi-Raymont, M. Cappi *et al.* Athena+: The first deep universe X-ray observatory. In *SF2A- 2013: Proceedings of the Annual Meeting of the French Society of Astronomy and Astrophysics*, edited by L. Cambresy, F. Martins, E. Nuss, and A. Palacios (2013), p. 447.
39. A. Merloni, P. Predehl, W. Becker, H. Böhringer, T. Boller, H. Brunner, M. Brusa, K. Dennerl, M. Freyberg, P. Friedrich *et al.* eROSITA science book: Mapping the structure of the energetic universe. e-prints http://adsabs.harvard.edu/abs/2012arXiv1209.3114M (2012).
40. S. Zane, D. Walton, T. Kennedy, M. Feroci, J.- W. Den Herder, M. Ahangarianabhari, A. Argan, P. Azzarello, G. Baldazzi, M. Barbera *et al.* The large area detector of LOFT: The large observatory for X-ray timing. in *Society of Photo-Optical Instrumentation Engineers (SPIE), Conference Series* (2014), vol. 9144, p. 2, 1408.6539.
41. A. Boyarsky, J. den Herder, A. Neronov, O. Ruchayskiy. Search for the light dark matter with an X-ray spectrometer. *Astroparticle Phys.* **28**, 303 (2007), astro-ph/0612219.
42. A. Boyarsky, D. Iakubovskyi, O. Ruchayskiy. Next decade of sterile neutrino studies. *Physics of the Dark Universe* **1**, 136 (2012).
43. A. Neronov, A. Boyarsky, D. Iakubovskyi, O. Ruchayskiy. Potential of the large observatory for X-ray timing tele-

scope for the search for dark matter. *Phys. Rev. D* **90**, 123532 (2014).

44. D. Iakubovskyi. Checking the potassium origin of the new emission line at 3.5 keV using the K XIX line complex at 3.7 keV. *Mon. Not. R. Astr. Soc.* **453**, 4097 (2015).
45. A. Neronov, D. Malyshev. Toward a full test of the ν MSM sterile neutrino dark matter model with Athena. *Phys. Rev. D* **93**, 063518 (2016).
46. F. Zandanel, C. Weniger, S. Ando. The role of the eROSITA all-sky survey in searches for sterile neutrino dark matter. *JCAP* **9**, 060 (2015).
47. A. Neronov, D. Malyshev, D. Eckert. Decaying dark matter search with NuSTAR deep sky observations. *Phys. Rev. D* **94**, 123504 (2016).
48. K. Perez, K.C.Y. Ng, J.F. Beacom, C. Hersh, S. Horiuchi, R. Krivonos. (Almost) Closing the νMSM sterile neutrino dark matter window with NuSTAR. *Phys. Rev. D* **95**, 123002 (2017).
49. F.A. Harrison, W.W. Craig, F.E. Christensen, C.J. Hailey, W.W. Zhang, S.E. Boggs, D. Stern, W.R. Cook, K. Forster, P. Giommi *et al.* The nuclear spectroscopic telescope array (NuSTAR) high-energy X-ray mission. *Astrophys. J.* **770**, 103 (2013).
50. K.A. Arnaud. XSPEC and PyXSPEC. In *AAS/High Energy Astrophysics Division* (2016), vol. 15, p. 115.02.
51. J.S. Kaastra, J.A.M. Bleeker. Optimal binning of X-ray spectra and response matrix design. *Astr. Astrophys.* **587**, A151 (2016).

Received 10.11.16

Д.О. Савченко, Д.А. Якубовський

ДО ПРОЦЕДУРИ ТОЧНОГО ПОШУКУ СЛАБКОЇ ВУЗЬКОЇ ЛІНІЇ В РЕНТГЕНІВСЬКОМУ СПЕКТРІ – РОЛЬ СИСТЕМАТИКИ, СПРИЧИНЕНОЇ МОДЕЛЮВАННЯМ КОНТИНУУМУ

Р е з ю м е

За деякими з недавніх детектувань вузької лінії випромінювання на ∼3,5 кеВ послідували дослідження, що показали відсутність лінії в тих самих джерелах. Це спричинило дискусії стосовно рівня систематичних похибок. В цій статті ми досліджуємо систематику, що спричинена недосконалим знанням моделі континууму. Проста теоретична оцінка та детальне моделювання симульованих спектрів дозволяють нам вперше визначити величину цієї систематичної похибки. Показано, що для деяких об'єктів з добре визначеною моделлю континууму, таким як галактика Андромеди, карликова сферична галактика Драко, отриманий рівень систематики дозволяє привести у відповідність спірні результати різних груп авторів. Показано, що для зменшення ефекту систематики, спричиненої моделюванням континуума, необхідно зменшувати розмір енергетичного біну в спектрі та збільшувати інтервал енергій при моделюванні.